Title

The Use of Synchrotron Radiation in the Medical Sciences

Journal

Photon science

ISSN

2998-8799

Authors

Osborn, Lydia
Inman, Jamie L
Ralston, Corie Y

Publication Date

2026-04-01

DOI

10.1021/photonsci.5c00051

Peer reviewed

PHOTON SCIENCE

pubs.acs.org/photonsci

Review

The Use of Synchrotron Radiation in the Medical Sciences

Lydia Osborn, Jamie L. Inman, and Corie Y. Ralston*

Cite This: https://doi.org/10.1021/photonsci.5c00051

Read Online

ACCESS | Metrics & More | Article Recommendations | Supporting Information

ABSTRACT: Synchrotron radiation (SR) sources provide unparalleled brilliance, collimation, coherence, and tunability, enabling specialized techniques that are crucial for advancing medical research across diverse fields from radiation oncology to rational drug design. Certain SR methods, such as macromolecular crystallography, are highly developed and automated, and have been used for decades for both fundamental understanding of biomolecules as well as pharmaceutical design, while other methods, such as microbeam radiation therapy, represent relatively recent developments. Scattering and diffraction methods using SR can provide atomic-level structural mapping of proteins, nucleic acids, and complexes. Imaging applications using SR continue to be developed and advanced for mapping of biological structures and potential use as diagnostics in disease detection. Spectroscopic methods are used to study elemental distributions relevant for detection of contamination in biological systems. Collectively, SR research delivers detailed multiscale structural and molecular information essential for addressing complex biomedical challenges. In this mini-review, we cover SR methods that are specifically relevant to medical applications, focusing mainly on SR X-ray and SR infrared techniques and applications. We include diffraction and scattering, imaging, absorption and fluorescent spectroscopy, use of SR in oncology treatments, and radiation damage methods that integrate one or another aspect of an SR method in conjunction with other non-SR techniques.

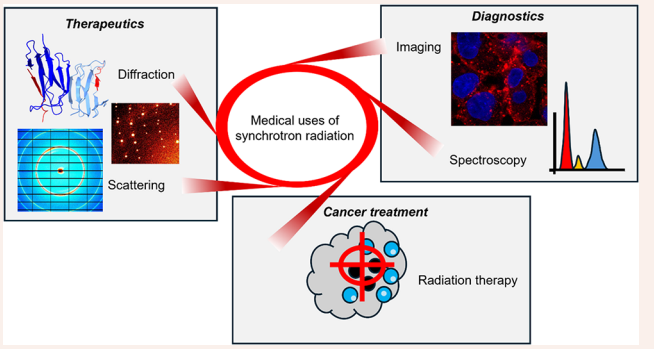

KEYWORDS: *synchrotron-based medical research, biomedical X-ray applications, radiation treatment, X-ray imaging, synchrotron facilities*

1. INTRODUCTION

Immediately after the discovery of X-ray radiation from a cathode ray tube in 1896,[1] scientists and medical researchers began to explore the use of X-rays for imaging and treatment of multiple diseases,[2] and in parallel, vacuum tube technology rapidly advanced to more efficiently produce brighter X-rays.[3] In the following decades, vacuum tubes were further developed for use in particle accelerators, and in the late 1940s, synchrotron X-ray radiation was first serendipitously observed as an unwanted byproduct of an electron accelerator.[4] In the following decades, synchrotron radiation became recognized as useful in its own right. Facilities producing synchrotron radiation continued to be developed in the 1950s, 60s, and 70s,[5,6] and the first dedicated facility optimized for producing synchrotron radiation (termed a second generation light source) was built in 1980.[7]

Today, the value of synchrotron radiation is widely recognized with several dozen facilities worldwide dedicated to producing photons in a range of wavelengths spanning X-rays to the infrared, and/or heavy ions or electrons. In the realm of X-rays, user-based synchrotron facilities are used in research fields from material characterization at the nanoscale to structural biology and radiation therapy. Many of these facilities continue to be developed to produce even brighter, smaller, and/or more coherent beams. The utility of synchrotron radiation is multifaceted. Its brightness and focusability to micron sized beams allows detection of minute quantities or impurities in materials at high spatial resolution. Its tunability enables absorption or transmission experiments with precise energies. Its coherence has enabled new types of imaging modalities such as coherent X-ray diffraction on the nanometer length scale,[8] while temporal studies can be conducted down to the picosecond time scale using pump-probe systems synchronized to the X-ray pulses produced by the synchrotron.[9] In addition, many synchrotron facilities support user programs, which enables access to those facilities and methods for scientists worldwide.

Previous review articles through the years[10−12] have covered the use and development of synchrotron radiation, often focusing on one field or specific application. Here, we review current developments in synchrotron radiation relevant for

Received: December 22, 2025
Revised: April 14, 2026
Accepted: April 14, 2026

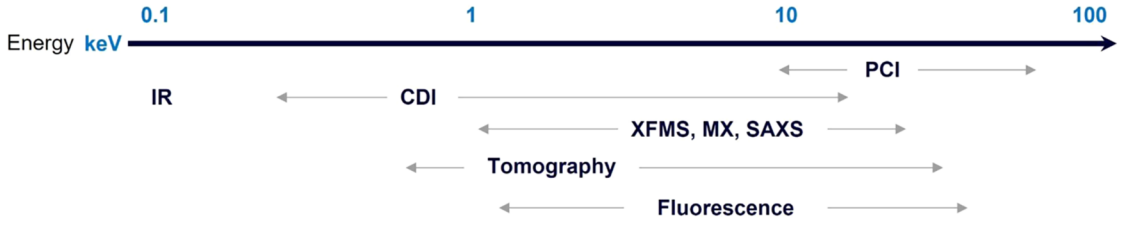

Method	IR	CDI	Tomography	XFMS	MX	PCI	SAXS	Fluorescence
Resolution	nm - μm	nm	μm - mm	Residue level	Angstrom	nm - μm	nm	nm - μm
Medical Applications	Dose detection, imaging	Imaging	Imaging	Epitope mapping, drug design	Drug design	Imaging	Drug design, biologic formulations	Imaging

Figure 1. Range of synchrotron methods used in biomedical applications, along with typical energy range, type of data collected, and resolution. CDI: coherent diffractive imaging, MX: macromolecular crystallography, PCI: Phase contrast imaging; SAXS: small angle X-ray scattering, XFMS: X-ray footprinting with mass spectrometry, IR: infrared.

medical sciences, including applications using both IR in the 100s of eV range, and X-rays ranging from several keV to 10 s of KeV energies (Figure 1). The applications cover fundamental research contributing to medical knowledge, such as protein structure determination, as well as practical applications using synchrotron radiation for radiotherapy in dosing and/or imaging. We have divided the article into four main sections: diffraction and scattering, imaging and spectroscopy, radiation treatment, and radiation damage methods. For each section, we discuss fundamental science and current and potential applications, and we conclude with a short overview of worldwide synchrotron X-ray facilities.

2. DIFFRACTION AND SCATTERING

Scattering of X-rays from materials results from interactions between the X-rays and the electrons in the material, which can be used to determine structural features of biological materials. In the special case of diffraction, the scattered light from a periodic structure of electrons interferes constructively or destructively to produce intensity rings (in the case of SAXS or WAXS) or distinct intensity spots (in the case of MX) on a detector. These patterns are unique to the biomolecule or complex being irradiated, and can be used to calculate structural information from the system at the sub-nanometer scale. Diffuse scattering from protein crystals has also been used to determine dynamics of proteins within crystals, although to a lesser extent.[13] Coherent X-ray diffractive imaging (CDI) is another diffraction-based method, in which coherent X-rays are used to irradiate a sample and the resulting diffraction patterns are used to reconstruct an image of the sample, typically at the 10s of nm level.[14] To obtain atomic level information, the wavelength of the X-rays should be on the order of the distance between atoms in the structure being irradiated. Modern synchrotron beamlines for MX typically supply peak X-ray wavelengths of around 1 Å at high photon flux density, and are also often focusable (or collimated) and tunable to a range of wavelengths.

2.1. Macromolecular Crystallography (MX) and Diffuse Scattering

The method of MX has a long history in determining structural properties of biological materials, with the first X-ray diffraction patterns from a protein crystal reported in the 1930s.[15] Not long after that, the first crystal structure of an antibiotic (penicillin) was reported[16] and the first protein structure was solved using X-ray diffraction in the late 1950s.[17] The availability of synchrotron X-rays beginning in the late 1960s and early 1970s subsequently had a dramatic effect on the throughput and resolution obtainable.[18] Today, most MX synchrotron beamlines worldwide are highly automated with robotic sample mounting, automated data collection, and automated data assessment, with throughput on the order of minutes per sample.[19] It should be noted that high brightness X-ray instruments are also commercially available and used for diffraction and scattering experiments, though do not typically have the user access or automation associated with synchrotron facilities. Protein crystal structures solved using MX are usually deposited in the worldwide protein data bank (PDB; https://www.rcsb.org/), which has had an enormous impact in biological research, both for general understanding of biological processes and for targeted drug design efforts. At a fundamental level, obtaining a protein structure is often a necessary step in understanding a biological process, since proteins serve in multiple roles in biological systems: as structural elements (e.g., complexes that give a cell structural integrity), decision-makers (e.g., gating the motion of molecules in and out of cells), and catalysts (e.g., breakdown of molecules or building of cellular structures). This fundamental understanding is then used in medical science applications, such as understanding disease mechanisms or design of antibodies. Pharmaceutical companies widely use MX to obtain protein structures as part of drug development efforts.[20] Small molecule crystallography is also used in pharmacological design since the crystal structure of a ligand or pharmaceutical ingredient can give information on stability, toxicity, and other characteristics relevant to drug design.[21] Further, PDB structures, primarily determined via MX though increasingly now through the method of CryoEM, were used to train AlphaFold,[22] a protein structure prediction program now widely used in many biological medical research areas. While diffuse scattering experiments have not led directly to protein structures, this type of data can nonetheless contribute to an understanding of protein dynamics within a structure, and can be collected as part of an MX experiment.[23]

https://doi.org/10.1021/photonsci.5c00051
Photon Sci. XXXX, XXX, XXX−XXX

2.2. Small Angle X-ray Scattering (SAXS)

As with MX, the development of SAXS dates back to the 1930s, and studies using the method to obtain low resolution structural features on biomolecules such as hemocyanine, actin, and myosin in solution were first performed in the 1940s and 1950s using X-ray tubes.[24,25] With the availability of synchrotron sources in the 1980s, the method gained traction and became more widely used for measuring proteins, protein complexes, protein-nucleic acid assemblies, and other biomolecules at several tens of Angstroms resolution.[26,27] The method has proved highly complementary to MX because it can provide structural information on biomolecule envelopes, conformational changes upon binding other proteins or ligands, and information on dynamics, all in the solution state. Today, SAXS at synchrotrons is important in several medical research areas. One area is in structural characterization of proteins, DNA/RNA, or complexes thereof relevant for drug design, such as SAXS characterization of the DNA or RNA forms recognized by HIV-1 reverse transcriptase.[28,29] Another growing area is in characterization of antibody-antigen complexes, which can be used to help optimize stability of an antibody, as well as help localize epitope/paratope regions.[30] This is particularly useful when combined with higher resolution methods such as MX. SAXS is also used in the pharmaceutical industry for quality control in biological formulations,[31] characterization of drug-delivery vehicles such as lipid nanoparticles to determine size distribution, investigation of the relationship between lipid content and stability and homogeneity,[32] or to provide structural information on viruses.[33] As with MX, the general structural information obtained by SAXS can be used for both fundamental understanding of biological systems and practical applications in drug design/optimization.

2.3. Coherent Diffractive Imaging (CDI)

CDI relies on diffraction from an object using a highly coherent beam, often without a focusing lens, to produce interference patterns which are then analyzed using phase-retrieval algorithms to produce an image of the object.[34,35] First proposed in 1980 as an extension of protein X-ray crystallography,[36] the method was not demonstrated using X-rays until the late 1990s.[37,38] CDI relies heavily on computational algorithms to derive an image and often uses scanning to produce many overlapping interference patterns, in which case the term ptychography is used to describe the method.[8,39−41] With scanning and fractionation, CDI can be applied using lower doses than the more standard methods of MX and SAXS, and thus can minimize radiation damage, often an important consideration for biological materials. Currently, synchrotron X-ray CDI methods are not in widespread use for direct biomedical applications, but have been used to gain fundamental understanding of biological systems such as actin filaments,[42] bacterial cells,[43−45] and fibroblasts.[46]

3. IMAGING AND SPECTROSCOPY

One of the earliest imaging applications of SR was the use of transvenous coronary angiography (TCA). Also referred to as dichromography or digital subtraction angiography in energy subtraction mode, TCA was an innovative medical technique developed to image the coronary arteries less invasively than traditional angiography. Initial studies were conducted on live patients in the 1980s and 90s at the Stanford Synchrotron Radiation Laboratory (SSRL) using a contrast agent (iodine-containing Renografin-76) administered intravenously through a catheter, and the scan acquisition was timed to bracket the moment the contrast agent filled the coronary circulation.[47] By 1995, a total of 7 human imaging sessions had been performed at SSRL/NSLS and 30 investigations had been performed at Hamburger Synchrotronstrahlungslabor (HASYLAB) using the NIKOS system.[48] The primary focus was on optimizing hardware (monochromators, detectors, scanners) and software to achieve images of sufficient quality for clinical relevance. SR provides the intense, continuous, and collimated beam necessary to create two quasi-monochromatic beams bracketing the iodine K-edge ($\Delta E \approx 300$ eV) which could be used for energy subtraction. This method allowed visualization of small iodinated structures, such as coronary arteries, after non-invasive intravenous injection.[48] However, despite the potential for non-invasive imaging, SR intensity must be very high to achieve good image resolution and the flux must be carefully controlled to stay within acceptable patient dose limits, which limits the resolution capability. Modern advancements in SR imaging have focused on phase contrast and dark field imaging methods, computed tomography methods, fluorescence, and infrared imaging on microscale structures. At the other end of the length scale, X-ray Absorption Spectroscopy (XAS) can be used to probe the local structural environment around an absorbing element, yielding subatomic distance information on nearest neighbors as well as the oxidation state of the absorbing element.

3.1. Phase Contrast and Dark Field Imaging

Synchtrotrons provide the small spot size and coherence that are advantageous for refraction based methods such as phase contrast and dark field imaging.[12] Phase contrast methods can also be incorporated into other methods such as tomography, as discussed here and in the next section.

In phase-contrast imaging (PCI) using synchrotron radiation allows for a spatial resolution at the micrometer level and a density resolution for light elements that is 1000 times higher than that of absorption-based imaging. Recently, PCI using in-line holography with synchrotron hard X-rays has been used to detect microscopic lesions on the cartilage of rabbit femoral heads.[49] PCI successfully visualized 20 μm micro-lesions on the cartilage surface which were completely invisible under conventional absorption-contrast X-ray imaging. Histological staining confirmed the presence of these lesions, suggesting that this non-invasive technique could serve as a powerful tool for the early diagnosis of osteoarthritis and cartilage degeneration.

A quantitative comparison between a clinical breast CT system and a synchrotron radiation (SR) breast CT setup utilizing a propagation-based phase-contrast technique with a photon-counting detector was performed in 2019.[50] Synchrotron radiation serves as a "gold standard" in this analysis due to its beam monochromaticity, which improves dose efficiency, and high coherence, which enables phase-contrast effects that enhance edge visibility and allow for phase-retrieval algorithms. The synchrotron system significantly outperforms the clinical system, achieving a spatial resolution of 5.0−6.7 lp/mm compared to 1.3 lp/mm for the clinical scanner, and a signal-to-noise ratio up to three times higher. Additionally, the synchrotron setup successfully detected significantly smaller diagnostic details, such as 0.15 mm fibers and 0.13 mm calcification clusters, which were not resolvable by the clinical system. X-ray phase-contrast tomography (XPCT) was also

https://doi.org/10.1021/photonsci.5c00051
Photon Sci. XXXX, XXX, XXX−XXX

used to analyze the 3D morphology and density of aortic walls in patients with acute type A aortic dissection (ATAAD), finding that while normal aortas exhibit homogeneous medial density, aortas from ATAAD patients without Marfan syndrome had significantly lower and inhomogeneous medial density.[51]

Synchrotron radiation is crucial for X-ray Dark-Field Imaging (XDFI) because its high spatial coherence allows for the direct resolution of intensity fringes and facilitates the tuning of autocorrelation lengths, while the monochromatic source eliminates the need for beam hardening corrections, making it ideal for imaging unstained structures, live cells, bacteria, or surface flaws. For example, Spindler et al. developed a system of dual-phase grating interferometers that generates Moiré fringes of tunable periods to measure dark-field signals without the photon-flux attenuation or cost associated with traditional analyzer gratings.[52] This setup successfully provides both absorption and dark-field images of porcine lungs and PMMA microspheres, achieving a sensitivity adequate for tracking lung micro-structures and suggesting the method's potential for diagnosing diseases like emphysema or fibrosis at low radiation doses. SR phase-contrast imaging was also employed to image human temporal bones and the surrounding tissues,[53] delineating a minimally invasive surgical pathway for delivering regenerative therapies directly to the cochlear nerve.

XDFI optics have also been combined with Refraction-Contrast Computed Tomography, specifically employing a Laue-type angle analyzer and a monochromator collimator to create 3D reconstructions of lung tissue. Yi et al. found that this technique clearly distinguished between primary and secondary lung adenocarcinomas based on their morphological features, such as spiculate margins in primary cancers versus smooth lobulated margins in metastatic ones.[54] Furthermore, the images correlated well with pathological examinations, successfully identifying features like ground-glass opacities and enabling precise 3D volumetric estimation of tumors without damaging the tissue.

3.2. Tomography

SR is a valuable source for micro or nano computed tomography (micro-CT or nano-CT) because it can provide highly coherent X-rays with high photon flux, which enables detailed, three-dimensional, non-destructive imaging of internal structures across various anatomical length scales.[55] Compared to classical imaging techniques such as TEM or SEM that require destructive sample processing, tomography's non-destructive nature allows samples to be imaged in their native context. This capability is invaluable to medical research because it allows for the high-resolution structural analysis of small, intricate biological components, such as in osteology research[56] as with middle ear ossicles,[57] or detailed neural networks,[58] or in validating novel medical implant micro-structures.[59]

SR tomography often incorporates phase-contrast imaging techniques, such as propagation-based phase-contrast SR, in-line phase-contrast imaging, or Zernike phase-contrast imaging, which utilize X-ray refraction to enhance the visibility and contrast of soft tissue boundaries and subtle density variations, sometimes by several orders of magnitude, without requiring contrast agents or complex sample preparation steps like sectioning.[55] For instance, Zernike phase plates have been successfully used with synchrotron X-ray nano-CT to image cellular components in mammalian tissues,[60] and to image nanoscale porosity structure in bone.[61] Similarly, Qi et al. utilized in-line phase-contrast synchrotron X-ray micro-CT to image a novel bone implant material,[59] and Handschuh et al. used micro-CT with staining and contrast agents to conduct mouse embryo disease phenotypes,[62] while Savatović et al. used modulation based micro-CT imaging study to complex vascular remodeling in organs like the lung and placenta.[63]

X-ray micro-CT provides in essence "virtual histology" in which a 3d image of a sample is created without physically sectioning a sample; however, it can also be used to guide traditional histology. Albers et al. developed this method to guide sectioning of heavy ion stained mouse lung tissue.[64] The types and usage of various histological stains are covered in other reviews.[65]

SR can also be applied to hard X-ray nanoholotomography (XNH) by merging traditional phase-contrast tomography with digital holography, allowing for the visualization of soft tissue density differences with nanoscale isotropic resolution (down to 88 nm) without the need for physical sectioning or staining. This technique was used on formalin-fixed paraffin-embedded human cerebellum and neocortex samples, successfully resolving hierarchical neuronal structures, including Purkinje and pyramidal cells, and visualizing subcellular features such as the nuclear envelope, nuclear pores, and nucleoli.[66] These virtual histology images correlated accurately with standard hematoxylin and eosin stained sections and allowed for the automated segmentation and morphometric analysis of individual neurons, demonstrating the potential of XNH for large-scale, non-destructive brain tissue characterization.

In conjunction with other methods, micro-CT can yield comprehensive structural information on biological samples, as in the interplay between osteosarcoma (OS), a malignant, heterogeneous bone tumor primarily affecting children and adolescents, and its tumor microenvironment (TME). For example, Rossi et al. characterized differences in osteosarcoma (OS) bone properties using X-ray computed microtomography, X-ray absorption spectroscopy, X-ray fluorescence microscopy, and X-ray diffraction to differentiate the three subtypes of OS by their mineralization and crystallinity,[67] specifically characterizing the distribution and structure of hydroxyapatite crystals, with applications in tracking disease progression and tailoring treatment for each subtype.

Staining methods have also been improved through the use of synchrotron radiation. A new staining method for human brain tissue that decreases tissue autolysis was validated using synchrotron microscopy. Post-mortem frozen human brain samples were subjected to a modified Golgi staining procedure for 30 days at near-freezing temperatures, and results were compared to traditional staining methods using SR micro-CT to evaluate the nuclear count, neuronal soma count, and dendritic spine density,[68] all measures of how well the neuronal integrity has been preserved. The ability of SR micro-CT to penetrate thick samples and yield high spatial resolution for complex neuronal structures in the cerebellum and frontal lobe enabled this staining method to be fully validated.

Speckle-based imaging (SBI) is an X-ray phase-contrast technique that uses simple random diffusers, such as abrasive sandpaper or filter membranes, to generate near-field speckle patterns acting as wavefront markers. Unlike Grating-Based Imaging (GBI), which relies on expensive high-precision gratings, SBI is more cost-effective and eliminates phase

https://doi.org/10.1021/photonsci.5c00051
Photon Sci. XXXX, XXX, XXX−XXX

unwrapping artifacts by employing real-space cross-correlation instead of Fourier domain analysis.[69,70] In terms of soft tissue, SBI has been used in conjunction with SR phase-contrast micro-CT for weakly absorbing soft tissue samples to show density variations within tissues such as the human placenta.[63] Highly coherent SR micro-CT was performed on unstained human placenta specimens to visualize its complex vascular structure, which is difficult to analyze non-destructively. SBI with sandpaper demonstrated the 3D virtual histology of the human placenta. SR-microCT was shown to provide comparable or superior information to conventional 2D histology, enabling deeper understanding of fetal development and associated placental disorders.

Micro-CT has also been used for live patient diagnostics. In 2024 researchers successfully used synchrotron-based micro-CT for biopsied vascular imaging in lung transplant patients, testing the effects of a mutation carrier vs a wild type transplant patient on vascular structures.[71] The high energy of SR gives it much better penetration than conventional radiation, allowing the imaging of thicker tissues taken from patients' lungs. The ability to 3D image microscale structural features has significant implications for the future of diagnostic methods; combined with spatially precise surgical and drug delivery techniques, it's part of the wave of targeting treatment on the microscale to reduce off-target effects and increase patient quality of life.

Synchrotron soft X-ray tomography (SXT) is a method that uses X-rays in a specific energy range − the "water window" between the carbon and oxygen absorption K-edges (282-533 eV) − where the carbon and nitrogen in biological molecules absorb an order of magnitude more strongly than water. The method can be used to image frozen cellular and subcellular structures down to ∼25 nm resolution.[72,73] Biomedical applications for this method are in the area of fundamental understanding of cellular function, dynamics, and/or morphology. Recent examples include a correlative microscopy methodology combining cryo-SXT and cryo-X-ray fluorescence mapping to analyze red blood cells infected with a malarial parasite.[74] Soft X-rays in the water window provided high-contrast 3D absorption images of cellular compartments like the parasite and digestive vacuole without staining, while hard X-ray nanobeams (17 keV) excited fluorescence to map elemental distributions of iron, sulfur, and potassium with high sensitivity. Cryo-SXT has also been used to visualize and quantify the morphological changes in red blood cells (RBCs) associated with Sickle Cell Disease (SCD) and to evaluate the efficacy of a therapeutic inhibitor, compound 5C.[75] Researchers reconstructed whole, fully hydrated RBCs at a resolution of approximately 50 nm without the need for sectioning or chemical fixation that could alter the native state.

3.3. Fluorescence Imaging

Fluorescence imaging has long been used for medical research because of its capacity to label and track specific molecules, organelles, cells, or tissues in both *in vivo* and *in vitro* conditions. Its specificity, tunability, and real-time dynamics make it a powerful tool for various medical research applications. Using SR as the source of X-rays for fluorescence microscopy increases the incident photon flux, resulting in higher sensitivity, measuring speed, and nanoscale spatial resolution, which allows researchers to measure quantitative distributions and concentrations of trace elements in biological samples without destroying the sample.[76] It can also be performed on non-conductive samples, which removes the surface charging artefacts and need for conductive coating that can restrict traditional electron-based microscopy on biological samples.[77] For example, synchrotron X-ray fluorescence microscopy (XFM) has been used to trace chemical elements and their spatial distribution in different types of microplastics at different stages of degradation.[78] The use of XFM enabled the researchers to illustrate the presence and, significantly, the internal spatial distribution of chemical elements (such as Ti, Zn, Cd, Cu, Cr, Sr, Fe, Br, and Pb) within the individual plastic fragments. XFM can detect and map the distribution of these potentially toxic elements with high spatial and temporal resolution in both organic and inorganic materials, with important implications for elucidating the metallome of disease models. Recently XFM was used to map the subcellular distribution of zinc, iron, and calcium in mouse pancreatic β-cells before and after immunofluorescence (IF) protocols,[79] revealing how the protocols disrupt calcium distribution and could be improved for better quantitative analysis of disease-relevant metallome phenotypes. The technique has potential to be used by researchers investigating how processing and degradation affects the structural makeup and cytotoxic effects of microparticles. Tracing the movement of contaminating surface modifications through their internalization into human cells could provide essential information on the mechanism of cellular uptake and on what types of microparticles are the most damaging.

3.4. Infrared Imaging

Synchrotron radiation infrared (SR-IR) sources are widely used for infrared spectromicroscopy and spectral imaging because they offer a brilliance two or three orders of magnitude higher than conventional thermal sources like a Globar. This exceptional brightness stems not from producing more total power, but from the intrinsically small source size and narrow angular emission of the synchrotron beams.[80] High brilliance enables superior signal-to-noise ratios, near diffraction limited spatial resolution, and rapid imaging of chemically heterogeneous biological samples.

IR spectroscopy provides molecule-specific vibrational signatures (biomolecular fingerprints) that report on protein secondary structure, lipid composition, and carbohydrate chemistry. When coupled with microscopy, IR enables highly resolved label-free chemical imaging of biomolecules in living individual cells without stains or fixatives.[80,81] This capability is valuable for probing dynamic biochemical processes such as apoptosis, necrosis, and cellular stress responses. Beyond cellular studies, IR spectromicroscopy holds promise for biomedical diagnostics, including the detection of basal cell carcinoma in skin and discrimination of disease-associated molecular phenotypes. Because IR microscopes are embedded within SR facilities, SR-IR measurements can also be integrated with complementary synchrotron-based modalities, most notably X-ray microscopy techniques such as X-ray fluorescence microscopy, on the same sample region. In addition, SR sources uniquely enable access to the far-IR region (TeraHertz domain) where conventional sources are limited, allowing investigation of collective excitations and protein conformational dynamics.[81]

Building on early pioneering demonstrations that established SR-IR spectromicroscopy for high-quality chemical imaging of individual living cells,[81,82] work by Holman and colleagues firmly positioned synchrotron IR spectromicroscopy as a

https://doi.org/10.1021/photonsci.5c00051
Photon Sci. XXXX, XXX, XXX−XXX

powerful, label-free approach for probing intrinsic cellular biochemistry with subcellular spatial resolution. Early studies demonstrated that mid-IR SR beams provide exceptional signal-to-noise with minimal heating or cytotoxicity, with no detectable loss of viability or biochemical perturbation during minutes-long measurements.[83] SR-based Fourier transform IR (SR-FTIR) spectromicroscopy further enabled quantitative resolution of biochemical signatures associated with cell cycle progression and cell death in individual living human fibroblasts, representing an early demonstration of live-cell chemical contrast using this modality.[84] Building on this foundation, SR-IR was applied to dissect dynamic molecular chemistry in living cells, capturing vibrational signatures of proteins, lipids, nucleic acids, and other biomolecules.[85,86] Importantly, this approach was extended to functional processes such as neuronal differentiation, where time-resolved spectral changes in single PC12 cells correlated with protein phosphorylation during nerve growth factor–induced differentiation, demonstrating real-time, label-free monitoring of post-translational signaling events.[87]

Collectively, this work established SR-IR spectromicroscopy as a uniquely powerful tool for revealing chemical heterogeneity and dynamic biochemical regulation at single-cell resolution. This capability has since been extended to a wide range of biomedical applications, including cancer biology, stem cell differentiation, neurobiology, and tissue pathology, supporting label-free investigation of disease-relevant biochemical states and cellular responses.[88−91]

3.5. X-ray Absorption Spectroscopy (XAS)

XAS generally requires high brightness X-rays and a tunable source, such as that from a synchrotron, to allow the energy of the incident X-rays to vary while detecting transmission through the sample, and/or fluorescence or emitted electrons.[92,93] Depending on the range of incident energies used, the method can be referred to as X-ray Absorption Near Edge Spectroscopy (XANES) or Extended X-ray Fine Structure Spectroscopy (EXAFS). The information obtained by XAS is somewhat limited, in that it provides structural, chemical, and/or geometry information only for the nearest coordinated atoms around the absorbing element.[94] However, the method can provide fundamental information relevant for biomedical applications,[95] such as in characterization of pharmaceuticals and in detection of metals in environmental or human samples. For example, XANES was used to measure the oxidation state of Pt within cisplatin cancer pharmaceuticals, which was relevant for characterizing the toxicity of the drugs.[96] In another example, the method was used to determine the spatial distribution of trace amounts of metals within human amyloid plaques derived from brain tissue.[97]

4. RADIATION TREATMENT

Synchrotron X-ray radiation is used both in fundamental studies to characterize dose and dose rate effects relevant to radiotherapy research, and in pre-clinical studies using high brightness X-ray sources directly for cancer treatment.[12] Synchrotron X-ray beamlines are capable of delivering very high dose rate radiation but can also be attenuated to reduce dose rate, allowing direct comparison between low and high dose rates, as is relevant for the FLASH studies described below. Preclinical studies have used highly collimated and/or focused high intensity synchrotron X-rays for testing microbeam irradiation of human tissues and animal models.[98]

4.1. FLASH Effect

The ability of ultra high dose rate (UHDR) radiation to increase cell survival was first observed in 1959 for bacteria irradiated with electrons and X-rays under various oxygenation conditions.[99] Dose rate studies on mammalian cells and tissue continued for several decades, and in 2014 the term "FLASH effect" was coined in a study showing the differential response of tumor and healthy tissue to high and low dose rate irradiation.[100] Now the phenomenon is well-defined; irradiating tissue at very high dose rates of hundreds or thousands of Grays per second (Gy/s; Gy = J/kg) maintains the tumor-killing properties of conventional radiotherapy (CONV-RT) but spares healthy tissue to a greater degree.[101] The potential for more effective cancer treatments using FLASH radiation therapy (FLASH-RT) has generated intense interest in radiation oncology, since the differential sparing of healthy tissue means that not only can tumors be treated more effectively, but also that the side-effects of radiation treatment can be minimized. The FLASH effect has been demonstrated repeatedly in cancers spanning 23 tumor types and multiple animal models,[101] using a variety of energy sources including electron, proton, and photon beams, and is currently in early clinical trials in humans.[102] However, the mechanism(s) behind the effect are still poorly understood,[103] which hinders accurate prediction of side effects and potential interactions with other therapies, as well as effective optimization of radiation treatments. One hypothesis is that rapid oxygen depletion caused by FLASH-RT creates a transiently hypoxic environment that reduces oxidative stress and DNA damage enough to spare healthy cells.[104] This hypothesis rests on the knowledge that tumor cells' high metabolism causes a buildup of reactive oxygen species (ROS), making them more sensitive to oxidative damage than healthy cells with a basal level of ROS. Therefore, investigating how proteins and DNA are differentially damaged by FLASH treatment in normoxic and hypoxic environments is crucial to determining if and how much transient oxygen depletion might be responsible for the FLASH effect. Another hypothesis is that radical–radical recombination in UHDR relative to CONV dose rates affects the final yields of ROS products. Other hypotheses rest on differential immune responses, preservation of specific organelles such as mitochondria, or cellular responses to DNA damage.

SR is an excellent source for investigating the FLASH effect since very high dose rates required are routinely achievable, while lower dose rates can also be studied using attenuation. Recent studies have been conducted to investigate the FLASH effect at synchrotron X-ray beamlines,[105,106] and FLASH platforms are being developed worldwide, including the Dresden Platform[107] in Germany for comparison of proton, electron, and γ radiation, and a peptide-based synchrotron radiation platform at the Advanced Light Source (ALS) in California.[103] In the latter, oxygen saturation can additionally be monitored inline, and oxidative modifications to proteins or peptides are measured using liquid chromatography mass spectrometry (LCMS). Using the ALS platform, results from analysis of peptide modifications showed a significant decrease in oxidative modifications under hypoxic conditions, as well as an approximately 50% decrease in modifications after a dose delivered by FLASH-RT compared to the same dose of CONV-RT.[103] In total, there was a 4-fold difference between the damage with normoxic CONV-RT and the damage with

https://doi.org/10.1021/photonsci.5c00051
Photon Sci. XXXX, XXX, XXX−XXX

hypoxic FLASH-RT, indicating that both dose rate and oxygen availability affect peptide radiation damage.

4.2. Microbeam Radiation Therapy

Microbeam radiation therapy (MRT) is another recent advancement in cancer radiotherapy that uses focused micrometer-scale X-ray beams to spatially target tumor cells and avoid exposing surrounding healthy tissue to radiation. SR is used to create a lattice of targeted parallel high dose rate microbeams alternating with gaps of low dose rate radiation, decreasing the treatment time needed and minimizing off-target irradiations.[98] The maximum doses possible using MRT are also much higher than CONV-RT because of their targeted nature. Instead of irradiating the entire body or a whole tissue, requiring repeated treatments of less-than-lethal doses for patient health, MRT allows for lethal doses of up to 1000 Gy to be delivered specifically to tumors. Preclinical studies show that MRT significantly minimizes radiation-induced lung damage, such as pulmonary fibrosis, compared to CONV-RT.[98] For example, 50 μm wide microbeams achieving peak doses of 600 Gy were shown to decrease tumor tissue while maintaining low fibrosis scores and minimal lung damage.[108] Furthermore, other studies using 50 μm wide microbeams observed the absence of microbeam path scarring in lung tissue 12 months post-irradiation,[109] suggesting effective lung tissue repair after micrometric high-dose damage. Despite the promising preclinical evidence that MRT can achieve local tumor control and minimize radiation-induced lung toxicity, its clinical translation is significantly hampered by the limited availability of specialized synchrotron research facilities worldwide. The heterogeneity in experimental setups and dosimetry reporting (e.g., peak doses, valley doses, and dose rates) across studies also presents a challenge to standardizing protocols necessary for clinical practice.

Recently Schültke et al. demonstrated the feasibility of microbeam irradiation for the treatment of adherent cultures of a radioresistant rodent melanoma cell line (F10B16).[110] They achieved an approximate 80% reduction of viable melanoma cell mass with a 50 μm beam and 400 μm spacing at a dose rate of approximately 70 Gy/s, potentially triggering the FLASH effect. Spatially fractioned MRT has also been combined with synchrotron broad beam radiation in an aggressive triple-negative breast cancer model (4T1.2 mouse mammary tumors).[111] The SR source provided kilovolt X-rays that were collimated into microbeams with 50 μm width and 200 μm spacing to deliver nonuniform doses; the peak doses were in the 100 to 500 Gy range, and valley doses of only a few Gy. Crucially, the synchrotron delivered these treatments at ultrahigh dose rates up to 6000 Gy/s, likely inducing FLASH effect conditions. They saw a substantially improved therapeutic ratio compared to CONV-RT and the SR-MRT induced specific local and systemic antitumor immune responses,[111] revealing its potential for treating even metastatic cancers. Furthermore, Engels et al. performed the first long-term MRT animal survival study at the Australian Synchrotron on intracerebral gliosarcoma (9LGS) bearing rats. They correlated *in vitro* cell response (using high dose rate fields to radiosensitize tumor cells) with *in vivo* survival and tumor dose coverage, successfully increasing lifespan by up to 570%.[112] Their results also confirmed with histological evidence that the normal brain tissue recovered over time, with only faint microbeam tracks distinguishable in the cured rat 72 weeks post-MRT, verifying the normal tissue sparing effect achievable with high-dose-rate SR delivery. These are only a few examples of the innovative ways in which MRT has been utilized in combination with synchrotron imaging and modeling to improve approaches to cancer treatment.

5. RADIATION DAMAGE METHODS

Synchrotron methods to study biomolecules are often used in conjunction with standard laboratory-based methods, such as fluorescence or absorption spectroscopy. Many MX beamlines, for instance, have integrated fluorescence detectors to measure metal content in protein crystal samples, while others provide additional photon sources for triggering structural changes within protein crystals during data collection.[113] For research areas in radiation damage, synchrotron irradiation can be followed by mass spectrometry analysis in solvent-accessibility structural studies, as with the method of X-ray footprinting mass spectrometry (XFMS). SR-IR sources, often combined with fluorescence readouts, can be used for characterization of subtle changes in tissues that have been irradiated using other modalities in a low dose regime, as described below for low dose detection.

5.1. X-ray Footprinting with Mass Spectrometry (XFMS)

XFMS is a relatively recently developed synchrotron structural biology method based on using solvent accessibility information to deduce protein structure.[114] In this method, synchrotron X-ray radiation radiolysis of an aqueous buffer produces hydroxyl radicals, which will modify protein side chains in solvent accessible regions. The resulting map of modifications is acquired through LCMS, and that map is used to determine regions where water is either present or occluded, which reveals ligand binding sites or sites of protein−protein interaction, and/or structural changes due to folding or unfolding. Using solvent accessibility to infer protein structure based on hydroxyl radical modification or enzymatic probes has a long history, but the first experiments to use synchrotron light for this method were conducted in the late 1990s at the National Synchrotron Light Source (NSLS) at Brookhaven National Laboratory.[115] The advantage of using a high brilliance X-ray source is that experiments can be conducted on a fast time scale which allows protein interaction events to be monitored at a sub-millisecond level. The limited time spent in the X-ray beam also reduces secondary oxidation events. Since that time, the method has grown in usage, and is often used to complement MX and SAXS studies, or in conjunction with biochemical or fluorescence based assays.[116,117] The method can help provide a fundamental understanding of protein structure, with specific medical applications in epitope/paratope mapping, antibody design or characterization, and small molecule binding. A recent example is the characterization of the interaction between the FDA-approved antibody Nivolumab and its target immune checkpoint receptor,[118] which contributed to understanding the basis of cancer immunotherapy treatments. Currently, there are two synchrotron XFMS facilities accessible through user programs, one at the ALS at Lawrence Berkeley National Lab[117] and one at the NSLS-II at Brookhaven National Laboratory.[119]

5.2. Low Dose Detection

Beyond high-dose and ultra-high-dose-rate radiotherapy paradigms, low-dose radiation biology remains a central and technically challenging area across radiobiology, radiation protection, and biomedical research. Biological responses in the ∼1 Gy and sub-Gy regime govern radiation risk assessment, normal-tissue tolerance, environmental and occupational exposure limits, space radiation effects, and the development of biodosimetry and medical countermeasures. Unlike high-dose effects, which often manifest as overt cell death or tissue injury, low-dose responses are frequently subtle, heterogeneous, and nonlinear, involving adaptive signaling, redox imbalance, metabolic reprogramming, and non-targeted effects that are difficult to capture using conventional morphological or survival-based end points.

SR provides a uniquely powerful platform for interrogating these low-dose regimes by combining precise dose and dose-rate control

https://doi.org/10.1021/photonsci.5c00051
Photon Sci. XXXX, XXX, XXX−XXX

Figure 2. World map showing locations of synchrotron facilities used in the reviewed research.

with high-sensitivity, label-free readouts of biochemical and cellular response. Synchrotron beamlines allow systematic comparison of dose, dose rate, and spatial heterogeneity within the same experimental framework, enabling mechanistic studies of low-dose radiation effects that are not readily accessible using conventional laboratory sources.

At the biochemical level, SR-FTIR spectromicroscopy has emerged as a sensitive, non-destructive modality for detecting radiation-induced changes that precede or occur independently of gross morphological damage. SR-FTIR has been applied to characterize radiation-dependent alterations in proteins, lipids, and nucleic acids following spatially fractionated irradiation paradigms.[120−122] These studies demonstrate that distinct vibrational signatures can report on stress responses across heterogeneous dose fields, revealing biochemical modulation even at low effective doses where conventional end points lack sensitivity. Because SR-FTIR employs low-energy mid-infrared photons that do not induce ionization, it is well suited for longitudinal and repeated measurements, enabling detection of low-dose exposure and delayed biochemical responses that are otherwise challenging to resolve.[123]

Mechanistic insight into low-dose radiation effects has also been advanced by SR X-ray microbeam irradiation at low doses, which allows energy deposition to be confined to specific cellular compartments with micrometer or sub-micrometer precision. Microbeam studies have demonstrated that bystander responses in the ∼1 Gy region depend strongly on the spatial location of energy deposition, with distinct outcomes observed when irradiation is targeted to the nucleus versus the whole cell.[124] Related work has revealed nonlinear bystander mutagenesis responses around ∼1 Gy, including reductions in mutation frequency under specific irradiation geometries, underscoring the complexity of low-dose, non-targeted effects.[125] These findings are supported by broader reviews highlighting SR microbeams as uniquely powerful tools for dissecting bystander and rescue phenomena, which are increasingly recognized as important contributors to tissue-level radiation response.[126,127]

In parallel with irradiation studies, SR facilities support dose-aware, high-information imaging modalities that balance sensitivity against radiation burden. Hard X-ray fluorescence microscopy (XFM) combined with phase-contrast imaging enables simultaneous mapping of elemental distributions and cellular morphology, allowing radiation-induced elemental redistribution to be evaluated within a structural context.[128] At still higher spatial resolution, coherent diffraction and ptychographic imaging have been applied to biological targets such as chromosomes, with explicit consideration of low-level irradiation and radiation damage constraints during measurement, emphasizing the importance of dose budgeting as resolution increases.[129]

Taken together, low-dose SR studies form a foundational pillar of modern radiation science, complementing high-dose radiotherapy advances while addressing questions that extend across risk assessment, normal-tissue biology, biodosimetry, and countermeasure development. By enabling precise irradiation control alongside sensitive, non-destructive readouts, SR platforms uniquely position low-dose radiation research to inform both fundamental biology and translational applications.

6. CONCLUDING REMARKS

There are currently several dozen synchrotron X-ray facilities worldwide (see, for instance, lightsources.org), many of which provide beamlines used for research in clinical applications or fundamental biomedical research, underscoring the importance of synchrotron radiation in the biomedical sciences. Table S1 lists the synchrotron facilities used for research we have discussed in this article. Some methods, such as MX, are considered routine and are highly automated, enabling remote access for ease of use; for these beamlines users typically send frozen protein crystals and control the beamline from off-site. These capabilities were especially useful during the recent COVID pandemic, in which onsite access was limited but protein structures were required for design of therapeutics. Other methods, such as MRT, are relatively recent and still under development, but show high promise for use in cancer treatment or diagnosis. Many synchrotron beamlines specialize in a given method, such as tomography, X-ray absorption, CDI, or SAXS, with a subset of projects devoted to biological samples. Examples of these include the Swiss Light Source TOMCAT beamline, optimized for dynamic X-ray imaging for time-resolved studies, the European Synchrotron Radiation Facility (ESRF) ID16A nanoimaging beamline, the SLS cSAXS beamline for coherent SAXS studies, and the Elettra

https://doi.org/10.1021/photonsci.5c00051
Photon Sci. XXXX, XXX, XXX−XXX

Synchrotron TwinMic beamline which provides dual fluorescence and transmission microscopy modes. A few beamlines are primarily focused on general medical research with wide-ranging technical capabilities, such as the Australian Synchrotron's Imaging and Medical Beamline, Elettra's Synchrotron Research for Medical Physics beamline, and the Biomedical Imaging and Therapy Facility (BMIT) beamline at the Canadian Light Source which developed a multiple energy imaging system using a polychromatic beam. Because synchrotrons provide a continuous and tunable energy range, beamlines can implement multispectral imaging methods in order to collect simultaneous structural and chemical information from samples and/or to reach a range of absorption edges for characterizing complex biological samples. These are only a few examples of the many facilities and beamlines used for the research reviewed here (Figure 2).

As synchrotron facilities continue to be upgraded to produce higher brightness sources, current capabilities will be enhanced and new applications will be made possible. For example, when NSLS was replaced with NSLS-II in 2014, the new diffraction and scattering beamlines were equipped with higher capacity, throughput, and resolution.[130,131] The Advanced Photon Source was recently upgraded to a multi-bend achromat ring and its beamlines are in the process of recommissioning,[132] while the ESRF ring and beamline upgrades were completed in 2022.[133] The current list of facility upgrade projects in progress or planned are too numerous to be listed here, but examples include the ALS, the Diamond Light Source, and SPring-8, which have planned upgrades due to be completed in the later part of this decade.

Despite the large cost of building and maintaining a synchrotron facility, many countries have invested in these facilities as national resources, and the fact that many go through continuous upgrades speaks to the importance of the science conducted at these facilities. Here we have reviewed the types of research and methods at synchrotron facilities in the biological sciences that bolster medical knowledge and lead to clinical applications.

■ ASSOCIATED CONTENT

Supporting Information

The Supporting Information is available free of charge at https://pubs.acs.org/doi/10.1021/photonsci.5c00051.

Table S1: Synchrotron facilities referenced in the article, with a list of associated biomedical research supported, and web addresses (PDF)

■ AUTHOR INFORMATION

Corresponding Author

Corie Y. Ralston − *Molecular Foundry Division, Lawrence Berkeley National Laboratory, Berkeley, California 94720, United States;* orcid.org/0000-0002-7899-0951; Email: cyralston@lbl.gov

Authors

Lydia Osborn − *Molecular Foundry Division, Lawrence Berkeley National Laboratory, Berkeley, California 94720, United States;* orcid.org/0009-0009-3806-8514

Jamie L. Inman − *Biological Systems and Engineering Division, Lawrence Berkeley National Laboratory, Berkeley, California 94720, United States;* orcid.org/0000-0002-6056-1219

Complete contact information is available at: https://pubs.acs.org/10.1021/photonsci.5c00051

Author Contributions

The manuscript was written through the contributions of all authors. All authors have given approval to the final version of the manuscript.

Notes

The authors declare no competing financial interest.

■ ACKNOWLEDGMENTS

Work is supported by the Laboratory Directed Research and Development funding under the U.S. Department of Energy Contract No. DE-AC02-05CH11231. The authors are grateful to colleagues at the Molecular Foundry for helpful conversations.

■ ABBREVIATIONS

CDI: coherent diffractive imaging; CT: computed tomography, IR, infrared; Micro-CT: micro-computed tomography; MX: macromolecular crystallography; SAXS: small angle X-ray scattering; XAS: X-ray absorption spectroscopy; XFMS: X-ray footprinting with mass spectrometry; XFM: X-ray fluorescence microscopy; PCI: phase contrast imaging

■ REFERENCES

(1) Röntgen, W. C. On a New Kind of Rays. *Nature* **1896**, *53* (1369), 274−276.

(2) Freund, L. Elements of General Radio-Therapy for Practitioners. *Nature* **1904**, *70* (1826), 624.

(3) Nascimento, M. L. F. Brief History of X-Ray Tube Patents. *World Pat. Inf.* **2014**, *37*, 48−53.

(4) Pollock, H. C. The Discovery of Synchrotron Radiation. *Am. J. Phys.* **1983**, *51* (3), 278−280.

(5) Tomboulian, D. H.; Hartman, P. L. Spectral and Angular Distribution of Ultraviolet Radiation from the 300-Mev Cornell Synchrotron. *Phys. Rev.* **1956**, *102* (6), 1423−1447.

(6) Rubloff, G. W.; Fritzsche, H.; Gerhardt, U.; Freeouf, J. Far Ultraviolet Spectroscopy of Solids in the Range 6−36 eV Using Synchrotron Radiation from an Electron Storage Ring. *Rev. Sci. Instrum.* **1971**, *42* (10), 1507−1513.

(7) Holder, D. J. The SRS at Daresbury Laboratory: A Eulogy to the World's First Dedicated High-Energy Synchrotron Radiation Source. In *Conf. Proc. C 0806233, Proceedings of the 11th European Conference, EPAC 2008,* Genoa, Italy, June 23−27, 2008 https://proceedings.jacow.org/e08/papers/wepc062.pdf.

(8) Thibault, P.; Guizar-Sicairos, M.; Menzel, A. Coherent Imaging at the Diffraction Limit. *J. Synchrotron Radiat.* **2014**, *21* (5), 1011−1018.

(9) Nozawa, S.; Adachi, S.; Takahashi, J.; Tazaki, R.; Guérin, L.; Daimon, M.; Tomita, A.; Sato, T.; Chollet, M.; Collet, E.; Cailleau, H.; Yamamoto, S.; Tsuchiya, K.; Shioya, T.; Sasaki, H.; Mori, T.; Ichiyanagi, K.; Sawa, H.; Kawata, H.; Koshihara, S. Developing 100 Ps-Resolved X-Ray Structural Analysis Capabilities on Beamline NW14A at the Photon Factory Advanced Ring. *J. Synchrotron Radiat.* **2007**, *14* (4), 313−319.

(10) Le Bas, J. F.; Charvet, A. M.; Elleaume, H.; Bertrand, B.; Esteve, F.; Spanne, P.; Suortti, P. A new X-ray source for medical imaging and radiotherapy research: synchrotron radiation. *Bull. Cancer* **1995**, *82* (Suppl 5), 544s−548s.

(11) Suortti, P.; Thomlinson, W. Medical Applications of Synchrotron Radiation. *Phys. Med. Biol.* **2003**, *48* (13), R1.

(12) Xiao, C.; Zhang, J.; Li, Y.; Xie, M.; Sun, D. Application of Synchrotron Radiation in Fundamental Research and Clinical Medicine. *Biomedicines* **2025**, *13* (6), 1419.

(13) Meisburger, S. P.; Case, D. A.; Ando, N. Diffuse X-Ray Scattering from Correlated Motions in a Protein Crystal. *Nat. Commun.* **2020**, *11* (1), No. 1271.
(14) Nave, C. The Achievable Resolution for X-Ray Imaging of Cells and Other Soft Biological Material. *IUCrJ* **2020**, *7* (Pt 3), 393−403.
(15) Bernal, J. D.; Crowfoot, D. X-Ray Photographs of Crystalline Pepsin. *Nature* **1934**, *133* (3369), 794−795.
(16) Hodgkin, D. C. The X-Ray Analysis of the Structure of Penicillin. *Adv. Sci.* **1949**, *6* (22), 85−89.
(17) Kendrew, J. C.; Dickerson, R. E.; Strandberg, B. E.; Hart, R. G.; Davies, D. R.; Phillips, D. C.; Shore, V. C. Structure of Myoglobin: A Three-Dimensional Fourier Synthesis at 2 Å. Resolution. *Nature* **1960**, *185* (4711), 422−427.
(18) Dauter, Z.; Jaskolski, M.; Wlodawer, A. Impact of Synchrotron Radiation on Macromolecular Crystallography: A Personal View. *J. Synchrotron Radiat.* **2010**, *17* (Pt 4), 433−444.
(19) Grabowski, M.; Cooper, D. R.; Brzezinski, D.; Macnar, J. M.; Shabalin, I. G.; Cymborowski, M.; Otwinowski, Z.; Minor, W. Synchrotron Radiation as a Tool for Macromolecular X-Ray Crystallography: A XXI Century Perspective. *Nucl. Instrum. Methods Phys. Res., Sect. B* **2021**, *489*, 30−40.
(20) Maveyraud, L.; Mourey, L. Protein X-Ray Crystallography and Drug Discovery. *Molecules* **2020**, *25* (5), 1030.
(21) Wouters, J.; Ooms, F. Small Molecule Crystallography in Drug Design. *Curr. Pharm. Des.* **2001**, *7* (7), 529−545.
(22) Jumper, J.; Evans, R.; Pritzel, A.; Green, T.; Figurnov, M.; Ronneberger, O.; Tunyasuvunakool, K.; Bates, R.; Žídek, A.; Potapenko, A.; Bridgland, A.; Meyer, C.; Kohl, S. A. A.; Ballard, A. J.; Cowie, A.; Romera-Paredes, B.; Nikolov, S.; Jain, R.; Adler, J.; Back, T.; Petersen, S.; Reiman, D.; Clancy, E.; Zielinski, M.; Steinegger, M.; Pacholska, M.; Berghammer, T.; Bodenstein, S.; Silver, D.; Vinyals, O.; Senior, A. W.; Kavukcuoglu, K.; Kohli, P.; Hassabis, D. Highly Accurate Protein Structure Prediction with AlphaFold. *Nature* **2021**, *596* (7873), 583−589.
(23) Wall, M. E.; Wolff, A. M.; Fraser, J. S. Bringing Diffuse X-Ray Scattering into Focus. *Curr. Opin. Struct. Biol.* **2018**, *50*, 109−116.
(24) Kratky, O.; Porod, G.; Sekora, A.; Paletta, B. Determination of the Shape of Gamma-Globulin by Means of the x-Ray Low-Angle Method. *J. Polym. Sci.* **1955**, *16* (82), 163−175.
(25) Kratky, O.; Porod, G. Diffuse Small-Angle Scattering of x-Rays in Colloid Systems. *J. Colloid Sci.* **1949**, *4* (1), 35−70.
(26) Meisburger, S. P.; Thomas, W. C.; Watkins, M. B.; Ando, N. X-Ray Scattering Studies of Protein Structural Dynamics. *Chem. Rev.* **2017**, *117* (12), 7615−7672.
(27) Franke, D.; Svergun, D. I. Synchrotron Small-Angle X-Ray Scattering on Biological Macromolecules in Solution. In *Synchrotron Light Sources and Free-Electron Lasers*; Springer: Cham, 2020; pp 1645−1672 DOI: 10.1007/978-3-030-23201-6_34.
(28) Fang, X.; Wang, J.; O'Carroll, I. P.; Mitchell, M.; Zuo, X.; Wang, Y.; Yu, P.; Liu, Y.; Rausch, J. W.; Dyba, M. A.; Kjems, J.; Schwieters, C. D.; Seifert, S.; Winans, R. E.; Watts, N. R.; Stahl, S. J.; Wingfield, P. T.; Byrd, R. A.; Le Grice, S. F. J.; Rein, A.; Wang, Y.-X. An Unusual Topological Structure of the HIV-1 Rev Response Element. *Cell* **2013**, *155* (3), 594−605.
(29) Tuske, S.; Zheng, J.; Olson, E. D.; Ruiz, F. X.; Pascal, B. D.; Hoang, A.; Bauman, J. D.; Das, K.; DeStefano, J. J.; Musier-Forsyth, K.; Griffin, P. R.; Arnold, E. Integrative Structural Biology Studies of HIV-1 Reverse Transcriptase Binding to a High-Affinity DNA Aptamer. *Curr. Res. Struct. Biol.* **2020**, *2*, 116−129.
(30) Castellanos, M. M.; Snyder, J. A.; Lee, M.; Chakravarthy, S.; Clark, N. J.; McAuley, A.; Curtis, J. E. Characterization of Monoclonal Antibody−Protein Antigen Complexes Using Small-Angle Scattering and Molecular Modeling. *Antibodies* **2017**, *6* (4), 25.
(31) Sonje, J.; Thakral, S.; Krueger, S.; Suryanarayanan, R. Enabling Efficient Design of Biological Formulations Through Advanced Characterization. *Pharm. Res.* **2023**, *40* (6), 1459−1477.
(32) Kim, L. J.; Shin, D.; Leite, W. C.; O'Neill, H.; Ruebel, O.; Tritt, A.; Hura, G. L. Simple Scattering: Lipid Nanoparticle Structural Data Repository. *Front. Mol. Biosci.* **2024**, *11*, No. 1321364, DOI: 10.3389/fmolb.2024.1321364.
(33) Khaykelson, D.; Raviv, U. Studying Viruses Using Solution X-Ray Scattering. *Biophys. Rev.* **2020**, *12* (1), 41−48.
(34) Faulkner, H. M. L.; Rodenburg, J. M. Movable Aperture Lensless Transmission Microscopy: A Novel Phase Retrieval Algorithm. *Phys. Rev. Lett.* **2004**, *93* (2), No. 023903.
(35) Chapman, H. N.; Nugent, K. A. Coherent Lensless X-Ray Imaging. *Nat. Photonics* **2010**, *4* (12), 833−839.
(36) Schlenker, M.; Fink, M.; Goedgebuer, J.-P.; Malgrange, C.; Viénot, J.; Wade, R. Imaging Processes and Coherence in Physics. *Proceedings of a workshop*; Centre de Physique: Les Houches, France, March 1979; DOI: 10.1007/3-540-09727-9.
(37) Chapman, H. N. Phase-Retrieval X-Ray Microscopy by Wigner-Distribution Deconvolution. *Ultramicroscopy* **1996**, *66* (3), 153−172.
(38) Miao, J.; Charalambous, P.; Kirz, J.; Sayre, D. Extending the Methodology of X-Ray Crystallography to Allow Imaging of Micrometre-Sized Non-Crystalline Specimens. *Nature* **1999**, *400* (6742), 342−344.
(39) Pfeiffer, F. X-Ray Ptychography. *Nat. Photonics* **2018**, *12* (1), 9−17.
(40) Rodenburg, J. M.; Hurst, A. C.; Cullis, A. G.; Dobson, B. R.; Pfeiffer, F.; Bunk, O.; David, C.; Jefimovs, K.; Johnson, I. Hard-X-Ray Lensless Imaging of Extended Objects. *Phys. Rev. Lett.* **2007**, *98* (3), No. 034801.
(41) Dierolf, M.; Bunk, O.; Kynde, S.; Thibault, P.; Johnson, I.; Menzel, A.; Jefimovs, K.; David, C.; Marti, O.; Pfeiffer, F. Ptychography & Lensless X-Ray Imaging. *Europhys. News* **2008**, *39* (1), 22−24.
(42) Piazza, V.; Weinhausen, B.; Diaz, A.; Dammann, C.; Maurer, C.; Reynolds, M.; Burghammer, M.; Köster, S. Revealing the Structure of Stereociliary Actin by X-Ray Nanoimaging. *ACS Nano* **2014**, *8* (12), 12228−12237.
(43) Giewekemeyer, K.; Thibault, P.; Kalbfleisch, S.; Beerlink, A.; Kewish, C. M.; Dierolf, M.; Pfeiffer, F.; Salditt, T. Quantitative Biological Imaging by Ptychographic X-Ray Diffraction Microscopy. *Proc. Natl. Acad. Sci. U.S.A.* **2010**, *107* (2), 529−534.
(44) Zhu, X.; Hitchcock, A. P.; Bazylinski, D. A.; Denes, P.; Joseph, J.; Lins, U.; Marchesini, S.; Shiu, H.-W.; Tyliszczak, T.; Shapiro, D. A. Measuring Spectroscopy and Magnetism of Extracted and Intracellular Magnetosomes Using Soft X-Ray Ptychography. *Proc. Natl. Acad. Sci. U.S.A.* **2016**, *113* (51), E8219−E8227.
(45) Diaz, A.; Malkova, B.; Holler, M.; Guizar-Sicairos, M.; Lima, E.; Panneels, V.; Pigino, G.; Bittermann, A. G.; Wettstein, L.; Tomizaki, T.; Bunk, O.; Schertler, G.; Ishikawa, T.; Wepf, R.; Menzel, A. Three-Dimensional Mass Density Mapping of Cellular Ultrastructure by Ptychographic X-Ray Nanotomography. *J. Struct. Biol.* **2015**, *192* (3), 461−469.
(46) Maiden, A. M.; Morrison, G. R.; Kaulich, B.; Gianoncelli, A.; Rodenburg, J. M. Soft X-Ray Spectromicroscopy Using Ptychography with Randomly Phased Illumination. *Nat. Commun.* **2013**, *4* (1), No. 1669.
(47) Rubenstein, E.; Hofstadter, R.; Zeman, H. D.; Thompson, A. C.; Otis, J. N.; Brown, G. S.; Giacomini, J. C.; Gordon, H. J.; Kernoff, R. S.; Harrison, D. C. Transvenous Coronary Angiography in Humans Using Synchrotron Radiation. *Proc. Natl. Acad. Sci. U.S.A.* **1986**, *83* (24), 9724−9728.
(48) Dix, W.-R. Intravenous Coronary Angiography with Synchrotron Radiation. *Prog. Biophys. Mol. Biol.* **1995**, *63* (2), 159−191.
(49) Sun, W.; Zhang, Y.; Gao, F.; Li, Z.; Li, G.; Pan, L. Phase-Contrast Imaging with Synchrotron Hard X-Ray of Micro Lesions of the Cartilage of the Femoral Head in Rabbits. *Int. J. Clin. Exp. Med.* **2015**, *8* (11), 20086−20091.
(50) Brombal, L.; Arfelli, F.; Delogu, P.; Donato, S.; Mettivier, G.; Michielsen, K.; Oliva, P.; Taibi, A.; Sechopoulos, I.; Longo, R.; Fedon, C. Image Quality Comparison between a Phase-Contrast Synchrotron Radiation Breast CT and a Clinical Breast CT: A Phantom Based Study. *Sci. Rep.* **2019**, *9* (1), No. 17778.

https://doi.org/10.1021/photonsci.5c00051
Photon Sci. XXXX, XXX, XXX−XXX

(51) Yokawa, K.; Hoshino, M.; Yagi, N.; Nakashima, Y.; Nakagawa, K.; Okita, Y.; Okada, K.; Tsukube, T. Synchrotron Radiation-Based X-Ray Phase-Contrast Imaging of the Aortic Walls in Acute Aortic Dissection. *JVS-Vasc. Sci.* **2020**, *1*, 81−91.
(52) Spindler, S.; Pereira, A.; Organista, C.; Zdora, M.-C.; Lovric, G.; Lautizi, G.; Dullin, C.; Contillo, A.; Longo, E.; Sodini, N.; D'Amico, L.; Romano, L.; Jefimovs, K.; Josell, D.; Rawlik, M.; Tromba, G.; Stampanoni, M. Synchrotron Radiation Based Analyzer-Free Dual-Phase Dark-Field Lung Imaging Approach for Radiography and CT. *Sci. Rep.* **2025**, *15* (1), No. 38615.
(53) Li, H.; Agrawal, S.; Zhu, N.; Cacciabue, D. I.; Rivolta, M. N.; Hartley, D. E. H.; Jiang, D.; Ladak, H. M.; O'Donoghue, G. M. Rask-Andersen, H. A Novel Therapeutic Pathway to the Human Cochlear Nerve. *Sci. Rep.* **2024**, *14* (1), No. 26795.
(54) Yi, E.; Sunaguchi, N.; Lee, J. H.; Seo, S.-J.; Lee, S.; Shimao, D.; Ando, M. Synchrotron Radiation Refraction-Contrast Computed Tomography Based on X-Ray Dark-Field Imaging Optics of Pulmonary Malignancy: Comparison with Pathologic Examination. *Cancers* **2024**, *16* (4), 806.
(55) Baruchel, J.; Buffiere, J.-Y.; Cloetens, P.; Di Michiel, M.; Ferrie, E.; Ludwig, W.; Maire, E.; Salvo, L. Advances in Synchrotron Radiation Microtomography. *Scr. Mater.* **2006**, *55* (1), 41−46.
(56) Obata, Y.; Bale, H. A.; Barnard, H. S.; Parkinson, D. Y.; Alliston, T.; Acevedo, C. Quantitative and Qualitative Bone Imaging: A Review of Synchrotron Radiation Microtomography Analysis in Bone Research. *J. Mech. Behav. Biomed. Mater.* **2020**, *110*, No. 103887.
(57) Ugarteburu, M.; Doube, M.; Witek, L.; Rau, C.; Cardoso, L.; Richter, C.-P.; Carriero, A. Small and Porous Ossicles, with Flat Stapes Footplate and Incudal Fractures in the *Oim* Mouse Model of Osteogenesis Imperfecta. *Bone* **2025**, *196*, No. 117495.
(58) Fonseca, M. de C.; Araujo, B. H. S.; Dias, C. S. B.; Archilha, N. L.; Neto, D. P. A.; Cavalheiro, E.; Westfahl, H.; da Silva, A. J. R.; Franchini, K. G. High-Resolution Synchrotron-Based X-Ray Micro-tomography as a Tool to Unveil the Three-Dimensional Neuronal Architecture of the Brain. *Sci. Rep.* **2018**, *8* (1), No. 12074.
(59) Qi, M.-l.; Li, M.; Yuan, K.; Song, E.; Zhang, H.; Yao, S. Fabrication and X-Ray Microtomography of Sandwich-Structured PEEK Implants for Skull Defect Repair. *Sci. Rep.* **2024**, *14* (1), No. 28585.
(60) Longo, E.; Sancey, L.; Flenner, S.; Kubec, A.; Bonnin, A.; David, C.; Müller, M.; Greving, I. X-Ray Zernike Phase Contrast Tomography: 3D ROI Visualization of Mm-Sized Mice Organ Tissues down to Sub-Cellular Components. *Biomed. Opt. Express* **2020**, *11* (10), 5506−5517.
(61) Silveira, A.; Greving, I.; Longo, E.; Scheel, M.; Weitkamp, T.; Fleck, C.; Shahar, R.; Zaslansky, P. Deep Learning to Overcome Zernike Phase-Contrast nanoCT Artifacts for Automated Micro-Nano Porosity Segmentation in Bone. *J. Synchrotron Radiat.* **2024**, *31* (1), 136−149.
(62) Handschuh, S.; Glösmann, M. Mouse Embryo Phenotyping Using X-Ray microCT. *Front. Cell Dev. Biol.* **2022**, *10*, No. 949184, DOI: 10.3389/fcell.2022.949184.
(63) Savatović, S.; Laundon, D.; De Marco, F.; Riedel, M.; Hammel, J. U.; Busse, M.; Salomé, M.; Pascolo, L.; Zanette, I.; Lewis, R. M.; Herzen, J.; Thibault, P. High-Resolution X-Ray Phase-Contrast Tomography of Human Placenta with Different Wavefront Markers. *Sci. Rep.* **2025**, *15* (1), No. 2131.
(64) Albers, J.; Markus, M. A.; Alves, F.; Dullin, C. X-Ray Based Virtual Histology Allows Guided Sectioning of Heavy Ion Stained Murine Lungs for Histological Analysis. *Sci. Rep.* **2018**, *8* (1), No. 7712.
(65) Javaeed, A.; Qamar, S.; Ali, S.; Mustafa, M. A. T.; Nusrat, A.; Ghauri, S. K. Histological Stains in the Past, Present, and Future. *Cureus* **2021**, No. 10, No. e18486.
(66) Khimchenko, A.; Bikis, C.; Pacureanu, A.; Hieber, S. E.; Thalmann, P.; Deyhle, H.; Schweighauser, G.; Hench, J.; Frank, S.; Müller-Gerbl, M.; Schulz, G.; Cloetens, P.; Müller, B. Hard X-Ray Nanoholotomography: Large-Scale, Label-Free, 3D Neuroimaging beyond Optical Limit. *Adv. Sci.* **2018**, *5* (6), No. 1700694.
(67) Rossi, F.; Rydzyk, M. M.; Barba, L.; Malucelli, E.; Palamà, M. E. F.; Gentili, C.; Mastrogiacomo, M.; Cedola, A.; Mancini, L.; Salomé, M.; Castillo-Michel, H.; Donati, D. M.; Gambarotti, M.; Lucarelli, E.; Fratini, M.; Iotti, S. Insights into the Osteosarcoma Microenvironment: Multiscale Analysis of Structural and Mineral Heterogeneity. *Acta Biomater.* **2025**, *199*, 193−201.
(68) Zhou, F.; Tang, Q.; Yan, X.; Ma, C.; Zhang, Y.; Zhang, J.; Li, Q.; Wang, L.; Hu, J.; Cai, X.; Li, J.; Zhu, Y.; Fan, C. Near-Freezing-Temperature Golgi Neuronal Staining for X-ray Imaging of Human Brain. *Adv. Sci.* **2025**, *12* (30), No. e04468.
(69) Kashyap, Y.; Wang, H.; Sawhney, K. Experimental Comparison between Speckle and Grating-Based Imaging Technique Using Synchrotron Radiation X-Rays. *Opt. Express* **2016**, *24* (16), 18664−18673.
(70) Celestre, R.; Quénot, L.; Ninham, C.; Brun, E.; Fardin, L. Review and Experimental Comparison of Speckle-Tracking Algorithms for X-Ray Phase Contrast Imaging. *J. Synchrotron Radiat.* **2025**, *32* (Pt 1), 180−199.
(71) Jeremiasen, I.; Peruzzi, N.; Lampei, E.; Meyer, S.; Akyürek, L. M.; Gebre-Medhin, E.; Mutgan, C.; Dorfmüller, P.; Neubert, L.; Jonigk, D.; Galambos, C.; Tran-Lundmark, K. Synchrotron-Based Phase-Contrast Micro-CT Combined With Histology to Decipher Differences Between Hereditary and Sporadic Pediatric Pulmonary Veno-Occlusive Disease. *Pulm. Circ.* **2024**, *14* (4), No. e70024.
(72) Okolo, C. A. A Guide into the World of High-Resolution 3D Imaging: The Case of Soft X-Ray Tomography for the Life Sciences. *Biochem. Soc. Trans.* **2022**, *50* (2), 649−663.
(73) Harkiolaki, M.; Darrow, M. C.; Spink, M. C.; Kosior, E.; Dent, K.; Duke, E. Cryo-Soft X-Ray Tomography: Using Soft X-Rays to Explore the Ultrastructure of Whole Cells. *Emerg. Top. Life Sci.* **2018**, *2* (1), 81−92.
(74) Kapishnikov, S.; Leiserowitz, L.; Yang, Y.; Cloetens, P.; Pereiro, E.; Awamu Ndonglack, F.; Matuschewski, K.; Als-Nielsen, J. Biochemistry of Malaria Parasite Infected Red Blood Cells by X-Ray Microscopy. *Sci. Rep.* **2017**, *7*, No. 802.
(75) Darrow, M. C.; Zhang, Y.; Cinquin, B. P.; Smith, E. A.; Boudreau, R.; Rochat, R. H.; Schmid, M. F.; Xia, Y.; Larabell, C. A.; Chiu, W. Visualizing Red Blood Cell Sickling and the Effects of Inhibition of Sphingosine Kinase 1 Using Soft X-Ray Tomography. *J. Cell Sci.* **2016**, *129* (18), 3511−3517.
(76) Pushie, M. J.; Sylvain, N. J.; Hou, H.; Hackett, M. J.; Kelly, M. E.; Webb, S. M. X-Ray Fluorescence Microscopy Methods for Biological Tissues. *Metallomics* **2022**, *14* (6), No. mfac032.
(77) Sala, S.; Rengefors, K.; Kiventerä, J.; Patanen, M.; Gefors, L.; Werdinius, C.; Winge, S.; Broberg, K.; Kalbfleisch, S.; Sigfridsson Clauss, K. Applications of X-Ray Fluorescence Microscopy with Synchrotron Radiation: From Biology to Materials Science. *Radiat. Phys. Chem.* **2025**, *229*, No. 112491.
(78) Lavers, J. L.; Howell, N. R.; Bond, A. L.; Howard, D. L.; de Jonge, M. D.; Puskar, L.; Banati, R. B. Elemental Analysis by Neutron Activation Analysis and Synchrotron X-Ray Fluorescence Microscopy of Ocean Plastics Ingested by Pelagic Seabirds. *J. Hazard. Mater.* **2025**, *494*, No. 138528.
(79) Slepchenko, K. G.; Chen, S.; Corbin, K. L.; Colvin, R. A.; Nunemaker, C. S. The Use of Synchrotron X-Ray Fluorescent Imaging to Study Distribution and Content of Elements in Chemically Fixed Single Cells: A Case Study Using Mouse Pancreatic Beta-Cells. *Metallomics* **2023**, *15* (2), No. mfad006.
(80) Marcelli, A.; Cricenti, A.; Kwiatek, W. M.; Petibois, C. Biological Applications of Synchrotron Radiation Infrared Spectro-microscopy. *Biotechnol. Adv.* **2012**, *30* (6), 1390−1404.
(81) Dumas, P.; Miller, L. Biological and Biomedical Applications of Synchrotron Infrared Microspectroscopy. *J. Biol. Phys.* **2003**, *29* (2-3), 201−218.
(82) Jamin, N.; Dumas, P.; Moncuit, J.; Fridman, W. H.; Teillaud, J.-L.; Carr, G. L.; Williams, G. P. Chemical Imaging of Living Cells by Synchrotron Infrared Microspectrometry. In *Accelerator-Based Infrared Sources and Applications*; SPIE, 1997; Vol. *3153*, pp 133−140 DOI: 10.1117/12.279380.

https://doi.org/10.1021/photonsci.5c00051
Photon Sci. XXXX, XXX, XXX−XXX

(83) Holman, H.-Y. N.; Martin, M. C.; McKinney, W. R. Tracking Chemical Changes in a Live Cell: Biomedical Applications of SR-FTIR Spectromicroscopy. *J. Spectrosc.* **2003**, *17* (2−3), No. 486940.
(84) Holman, H. Y.; Martin, M. C.; Blakely, E. A.; Bjornstad, K.; McKinney, W. R. IR Spectroscopic Characteristics of Cell Cycle and Cell Death Probed by Synchrotron Radiation Based Fourier Transform IR Spectromicroscopy. *Biopolymers* **2000**, *57* (6), 329−335.
(85) Holman, H.-Y. N.; Bechtel, H. A.; Hao, Z.; Martin, M. C. Synchrotron IR Spectromicroscopy: Chemistry of Living Cells. *Anal. Chem.* **2010**, *82* (21), 8757−8765.
(86) Holman, H.-Y. N.; Bjornstad, K.; McNamara, M. P.; Martin, M. C.; McKinney, W. R.; Blakely, E. A. Synchrotron Infrared Spectromicroscopy as a Novel Bioanalytical Microprobe for Individual Living Cells: Cytotoxicity Considerations. *J. Biomed. Opt.* **2002**, *7* (3), 417−424.
(87) Chen, L.; Holman, H.-Y. N.; Hao, Z.; Bechtel, H. A.; Martin, M. C.; Wu, C.; Chu, S. Synchrotron Infrared Measurements of Protein Phosphorylation in Living Single PC12 Cells during Neuronal Differentiation. *Anal. Chem.* **2012**, *84* (9), 4118−4125.
(88) Kelly, J. G.; Singh, M. N.; Stringfellow, H. F.; Walsh, M. J.; Nicholson, J. M.; Bahrami, F.; Ashton, K. M.; Pitt, M. A.; Martin-Hirsch, P. L.; Martin, F. L. Derivation of a Subtype-Specific Biochemical Signature of Endometrial Carcinoma Using Synchrotron-Based Fourier-Transform Infrared Microspectroscopy. *Cancer Lett.* **2009**, *274* (2), 208−217.
(89) Dučić, T.; Rodriguez-Yañez, F.; Gonzalez-Muñoz, E. Synchrotron Radiation FTIR Microspectroscopy Enables Measuring Dynamic Cell Identity Patterning during Human 3D Differentiation. *Front. Cell Dev. Biol.* **2025**, *13*, No. 1569187, DOI: 10.3389/fcell.2025.1569187.
(90) Qian, J.; Gao, X.; Wang, Y.-D.; Li, X.-L.; Hu, J.; Lü, J.-H. Synchrotron Infrared Microspectroscopy for Stem Cell Research. *Int. J. Mol. Sci.* **2022**, *23* (17), 9878.
(91) Miller, L. M.; Dumas, P. Chemical Imaging of Biological Tissue with Synchrotron Infrared Light. *Biochim. Biophys. Acta, Biomembr.* **2006**, *1758* (7), 846−857.
(92) Fan, Y.; Wang, X.; Bo, G.; Xu, X.; See, K. W.; Johannessen, B.; Pang, W. K. Operando Synchrotron X-Ray Absorption Spectroscopy: A Key Tool for Cathode Material Studies in Next-Generation Batteries. *Adv. Sci.* **2025**, *12* (10), No. 2414480.
(93) Pongpiachan, S.; Thumanu, K.; Tanthanuch, W.; Srisamut, D.; Pradabsri, J.; Hashmi, M. Z.; Sun, Y.; Poshyachinda, S. Using Synchrotron Based ATR-FTIR, EXAFS, and XRF to Characterize the Chemical Compositions of TSP in Industrial Estate Area. *Heliyon* **2024**, *10* (20), No. e39215.
(94) Yano, J.; Yachandra, V. K. X-Ray Absorption Spectroscopy. *Photosynth. Res.* **2009**, *102* (2), 241−254.
(95) Guilherme Buzanich, A. Recent Developments of X-Ray Absorption Spectroscopy as Analytical Tool for Biological and Biomedical Applications. *X-Ray Spectrom.* **2022**, *51* (3), 294−303.
(96) Hall, M. D.; Daly, H. L.; Zhang, J. Z.; Zhang, M.; Alderden, R. A.; Pursche, D.; Foran, G. J.; Hambley, T. W. Quantitative Measurement of the Reduction of Platinum(Iv) Complexes Using X-Ray Absorption Near-Edge Spectroscopy (XANES). *Metallomics* **2012**, *4* (6), 568.
(97) Everett, J.; Lermyte, F.; Brooks, J.; Tjendana-Tjhin, V.; Plascencia-Villa, G.; Hands-Portman, I.; Donnelly, J. M.; Billimoria, K.; Perry, G.; Zhu, X.; Sadler, P. J.; O'Connor, P. B.; Collingwood, J. F.; Telling, N. D. Biogenic Metallic Elements in the Human Brain? *Sci. Adv.* **2021**, *7* (24), No. eabf6707.
(98) Reynolds, A.; Marignol, L. Microbeam Radiation Therapy for Lung Cancer: A Review of Experimental Setups and Biological Endpoints in Preclinical Studies. *Int. J. Radiat. Biol.* **2025**, *101* (6), 549−558.
(99) Dewey, D. L.; Boag, J. W. Modification of the Oxygen Effect When Bacteria Are given Large Pulses of Radiation. *Nature* **1959**, *183* (4673), 1450−1451.
(100) Favaudon, V.; Caplier, L.; Monceau, V.; Pouzoulet, F.; Sayarath, M.; Fouillade, C.; Poupon, M.-F.; Brito, I.; Hupé, P.; Bourhis, J.; Hall, J.; Fontaine, J.-J.; Vozenin, M.-C. Ultrahigh Dose-Rate FLASH Irradiation Increases the Differential Response between Normal and Tumor Tissue in Mice. *Sci. Transl. Med.* **2014**, *6* (245), 245−293.
(101) Limoli, C. L.; Vozenin, M.-C. Reinventing Radiobiology in the Light of FLASH Radiotherapy. *Annu. Rev. Cancer Biol.* **2023**, *7* (1), 1−21.
(102) Gaide, O.; Herrera, F.; Sozzi, W. J.; Jorge, P. G.; Kinj, R.; Bailat, C.; Duclos, F.; Bochud, F.; Germond, J.-F.; Gondré, M.; Boelhen, T.; Schiappacasse, L.; Ozsahin, M.; Moeckli, R.; Bourhis, J. Comparison of Ultra-High versus Conventional Dose Rate Radiotherapy in a Patient with Cutaneous Lymphoma. *Radiother. Oncol.* **2022**, *174*, 87−91.
(103) Gupta, S.; Inman, J. L.; De Chant, J.; Obst-Huebl, L.; Nakamura, K.; Costello, S. M.; Marqusee, S.; Mao, J.-H.; Kunz, L.; Paisley, R.; Vozenin, M.-C.; Snijders, A. M.; Ralston, C. Y. A Novel Platform for Evaluating Dose Rate Effects on Oxidative Damage to Peptides: Toward a High-Throughput Method to Characterize the Mechanisms Underlying the FLASH Effect. *Radiat. Res.* **2023**, *200* (6), 523−530.
(104) Cooper, C. R.; Jones, D.; Jones, G. D.; Petersson, K. FLASH Irradiation Induces Lower Levels of DNA Damage Ex Vivo, an Effect Modulated by Oxygen Tension, Dose, and Dose Rate. *Br. J. Radiol.* **2022**, *95* (1133), No. 20211150.
(105) Smyth, L. M. L.; Donoghue, J. F.; Ventura, J. A.; Livingstone, J.; Bailey, T.; Day, L. R. J.; Crosbie, J. C.; Rogers, P. A. W. Comparative Toxicity of Synchrotron and Conventional Radiation Therapy Based on Total and Partial Body Irradiation in a Murine Model. *Sci. Rep.* **2018**, *8* (1), No. 12044.
(106) Montay-Gruel, P.; Bouchet, A.; Jaccard, M.; Patin, D.; Serduc, R.; Aim, W.; Petersson, K.; Petit, B.; Bailat, C.; Bourhis, J.; Bräuer-Krisch, E.; Vozenin, M.-C. X-Rays Can Trigger the FLASH Effect: Ultra-High Dose-Rate Synchrotron Light Source Prevents Normal Brain Injury after Whole Brain Irradiation in Mice. *Radiother. Oncol.* **2018**, *129* (3), 582−588.
(107) Metzkes-Ng, J.; Brack, F.-E.; Kroll, F.; Bernert, C.; Bock, S.; Bodenstein, E.; Brand, M.; Cowan, T. E.; Gebhardt, R.; Hans, S.; Helbig, U.; Horst, F.; Jansen, J.; Kraft, S. D.; Krause, M.; Leßmann, E.; Löck, S.; Pawelke, J.; Püschel, T.; Reimold, M.; Rehwald, M.; Richter, C.; Schlenvoigt, H.-P.; Schramm, U.; Schürer, M.; Seco, J.; Szabó, E. R.; Umlandt, M. E. P.; Zeil, K.; Ziegler, T.; Beyreuther, E. The Dresden Platform Is a Research Hub for Ultra-High Dose Rate Radiobiology. *Sci. Rep.* **2023**, *13* (1), No. 20611.
(108) Wright, M. D.; Romanelli, P.; Bravin, A.; Duc, G. L.; Brauer-Krisch, E.; Requardt, H.; Bartzsch, S.; Hlushchuk, R.; Laissue, J.-A.; Djonov, V.; Wright, M. D.; Romanelli, P.; Bravin, A.; Duc, G. L.; Brauer-Krisch, E.; Requardt, H.; Bartzsch, S. H.; Hlushchuk, R.; Laissue, J.-A.; Djonov, V. Non-Conventional Ultra-High Dose Rate (FLASH) Microbeam Radiotherapy Provides Superior Normal Tissue Sparing in Rat Lung Compared to Non-Conventional Ultra-High Dose Rate (FLASH) Radiotherapy. *Cureus* **2021**, *13* (11), No. e19317, DOI: 10.7759/cureus.19317.
(109) Romano, M.; Bravin, A.; Wright, M. D.; Jacques, L.; Miettinen, A.; Hlushchuk, R.; Dinkel, J.; Bartzsch, S.; Laissue, J. A.; Djonov, V.; Coan, P. X-Ray Phase Contrast 3D Virtual Histology: Evaluation of Lung Alterations After Microbeam Irradiation. *Int. J. Radiat. Oncol.* **2022**, *112* (3), 818−830.
(110) Schültke, E.; Fiedler, S.; Menk, R. H.; Jaekel, F.; Dreossi, D.; Casarin, K.; Tromba, G.; Bartzsch, S.; Kriesen, S.; Hildebrandt, G.; Arfelli, F. Perspectives for Microbeam Irradiation at the SYRMEP Beamline. *J. Synchrotron Radiat.* **2021**, *28* (Pt 2), 410−418.
(111) Engels, E.; Forrester, H.; Klein, M.; Bell, C.; Balderstone, I.; Brunt, K.; Barnes, M. J.; Cameron, M.; Crosbie, J. C.; Middleton, R.; Fernandez-Palomo, C.; Dietler, B. de B.; Trappetti, V.; Fazzari, J. M.; Hausermann, D.; Anderson, R. L.; Djonov, V. G.; Martin, O. A. The Impact of Synchrotron Microbeam Radiation Therapy Combined With Broad Beam in a Preclinical Breast Cancer Model. *Adv. Radiat. Oncol.* **2025**, *10* (1), No. 101680.

https://doi.org/10.1021/photonsci.5c00051
Photon Sci. XXXX, XXX, XXX−XXX

(112) Engels, E.; Li, N.; Davis, J.; Paino, J.; Cameron, M.; Dipuglia, A.; Vogel, S.; Valceski, M.; Khochaiche, A.; O'Keefe, A.; Barnes, M.; Cullen, A.; Stevenson, A.; Guatelli, S.; Rosenfeld, A.; Lerch, M.; Corde, S.; Tehei, M. Toward Personalized Synchrotron Microbeam Radiation Therapy. *Sci. Rep.* **2020**, *10* (1), No. 8833.

(113) Aller, P.; Orville, A. M. Dynamic Structural Biology Experiments at XFEL or Synchrotron Sources. In *Structural Proteomics*; Owens, R. J., Ed.; Springer US: New York, NY, 2021; Vol. *2305*, pp 203−228 DOI: 10.1007/978-1-0716-1406-8_11.

(114) Xu, G.; Chance, M. R. Hydroxyl Radical-Mediated Modification of Proteins as Probes for Structural Proteomics. *Chem. Rev.* **2007**, *107* (8), 3514−3543.

(115) Sclavi, B.; Sullivan, M.; Chance, M. R.; Brenowitz, M.; Woodson, S. A. RNA Folding at Millisecond Intervals by Synchrotron Hydroxyl Radical Footprinting. *Science* **1998**, *279* (5358), 1940−1943.

(116) Gupta, S.; Russell, B.; Kristensen, L. G.; Tyler, J.; Costello, S. M.; Marqusee, S.; Rad, B.; Ralston, C. Y. Enabling Simultaneous Photoluminescence Spectroscopy and X-Ray Footprinting Mass Spectrometry to Study Protein Conformation and Interactions. *Anal. Methods* **2025**, *17* (6), 1214−1225.

(117) Ralston, C. Y.; Gupta, S.; Del Mundo, J. T.; Soe, A. C.; Russell, B.; Rad, B.; Tyler, J.; Paul, S.; Kahan, D. N.; Kristensen, L. G.; Subramanian, S.; Kidd, S.; Burnett, K.; Sankaran, B.; Classen, S.; Prigozhin, D. M.; Taylor, J. R.; Dickert, J. M.; Royal, K. B.; Rozales, A.; Ortega, S. L.; Allaire, M.; Nix, J. C.; Hura, G. L.; Holton, J. M.; Hammel, M.; Adams, P. D. ALS-ENABLE: Creating Synergy and Opportunity at the Advanced Light Source Synchrotron Structural Biology Beamlines. *J. Synchrotron Radiat.* **2025**, *32* (4), 1059−1067.

(118) Kristensen, L. G.; Gupta, S.; Chen, Y.; Petzold, C. J.; Ralston, C. Y. Residue-Specific Epitope Mapping of the PD-1/Nivolumab Interaction Using X-Ray Footprinting Mass Spectrometry. *Antibodies* **2024**, *13* (3), 77.

(119) Asuru, A.; Farquhar, E. R.; Sullivan, M.; Abel, D.; Toomey, J.; Chance, M. R.; Bohon, J. The XFP (17-BM) Beamline for X-Ray Footprinting at NSLS-II. *J. Synchrotron Radiat.* **2019**, *26* (4), 1388−1399.

(120) González-Vegas, R.; Yousef, I.; Seksek, O.; Ortiz, R.; Bertho, A.; Juchaux, M.; Nauraye, C.; Marzi, L. D.; Patriarca, A.; Prezado, Y.; Martínez-Rovira, I. Investigating the Biochemical Response of Proton Minibeam Radiation Therapy by Means of Synchrotron-Based Infrared Microspectroscopy. *Sci. Rep.* **2024**, *14* (1), No. 11973.

(121) González-Vegas, R.; Seksek, O.; Bertho, A.; Bergs, J.; Hirayama, R.; Inaniwa, T.; Matsufuji, N.; Shimokawa, T.; Prezado, Y.; Yousef, I.; Martínez-Rovira, I. Synchrotron-Based Infrared Microspectroscopy Unveils the Biomolecular Response of Healthy and Tumour Cell Lines to Neon Minibeam Radiation Therapy. *Analyst* **2025**, *150* (2), 342−352.

(122) Lipiec, E.; Birarda, G.; Kowalska, J.; Lekki, J.; Vaccari, L.; Wiecheć, A.; Wood, B. R.; Kwiatek, W. M. A New Approach to Studying the Effects of Ionising Radiation on Single Cells Using FTIR Synchrotron Microspectroscopy. *Radiat. Phys. Chem.* **2013**, *93*, 135−141.

(123) Inman, J. L.; Wu, Y.; Chen, L.; Brydon, E.; Ghosh, D.; Wan, K. H.; De Chant, J.; Obst-Huebl, L.; Nakamura, K.; Ralston, C. Y.; Celniker, S. E.; Mao, J.-H.; Zwart, P. H.; Holman, H.-Y. N.; Chang, H.; Brown, J. B.; Snijders, A. M. Long-Term, Non-Invasive FTIR Detection of Low-Dose Ionizing Radiation Exposure. *Sci. Rep.* **2024**, *14* (1), No. 6119.

(124) Maeda, M.; Tomita, M.; Usami, N.; Kobayashi, K. Bystander Cell Death Is Modified by Sites of Energy Deposition within Cells Irradiated with a Synchrotron X-Ray Microbeam. *Radiat. Res.* **2010**, *174* (1), 37−45.

(125) Maeda, M.; Kobayashi, K.; Matsumoto, H.; Usami, N.; Tomita, M. X-Ray-Induced Bystander Responses Reduce Spontaneous Mutations in V79 Cells. *J. Radiat. Res.* **2013**, *54* (6), 1043−1049.

(126) Prise, K. M.; Schettino, G.; Vojnovic, B.; Belyakov, O.; Shao, C. Microbeam Studies of the Bystander Response. *J. Radiat. Res.* **2009**, *50* (Suppl A), A1−A6.

(127) Brenner, D. J. Proceedings of the 7th International Workshop: Microbeam Probes of Cellular Radiation Response. *Radiat. Res.* **2006**, *166* (4), 652−689, DOI: 10.1667/RR0683.1.

(128) Kosior, E.; Bohic, S.; Suhonen, H.; Ortega, R.; Devès, G.; Carmona, A.; Marchi, F.; Guillet, J. F.; Cloetens, P. Combined Use of Hard X-Ray Phase Contrast Imaging and X-Ray Fluorescence Microscopy for Sub-Cellular Metal Quantification. *J. Struct. Biol.* **2012**, *177* (2), 239−247.

(129) Bhartiya, A.; Batey, D.; Cipiccia, S.; Shi, X.; Rau, C.; Botchway, S.; Yusuf, M.; Robinson, I. K. X-Ray Ptychography Imaging of Human Chromosomes After Low-Dose Irradiation. *Chromosome Res.* **2021**, *29* (1), 107−126.

(130) Barbour, A.; Cai, Y. Q.; Fluerasu, A.; Freychet, G.; Fukuto, M.; Gang, O.; Gann, E.; Laasch, R.; Li, R.; Ocko, B. M.; Tsai, E. H. R.; Wąsik, P.; Wiegart, L.; Yager, K. G.; Yang, L.; Zhang, H.; Zhang, Y. X-Ray Scattering for Soft Matter Research at NSLS-II. *Synchrotron Radiat. News* **2023**, *36* (2), 24−30.

(131) Schneider, D. K.; Soares, A. S.; Lazo, E. O.; Kreitler, D. F.; Qian, K.; Fuchs, M. R.; Bhogadi, D. K.; Antonelli, S.; Myers, S. S.; Martins, B. S.; Skinner, J. M.; Aishima, J.; Bernstein, H. J.; Langdon, T.; Lara, J.; Petkus, R.; Cowan, M.; Flaks, L.; Smith, T.; Shea-McCarthy, G.; Idir, M.; Huang, L.; Chubar, O.; Sweet, R. M.; Berman, L. E.; McSweeney, S.; Jakoncic, J. AMX − the Highly Automated Macromolecular Crystallography (17-ID-1) Beamline at the NSLS-II. *J. Synchrotron Radiat.* **2022**, *29* (6), 1480−1494.

(132) Shi, X.; Lin, Y.-C.; Zhao, J.; Toellner, T.; Hu, M. Y.; Seifert, S.; Lee, B.; Grizolli, W.; Wojcik, M. J.; Rebuffi, L.; Assoufid, L.; Sajaev, V. Measurements of Source Emittance and Beam Coherence Properties of the Upgraded Advanced Photon Source. *J. Synchrotron Radiat.* **2025**, *32* (5), 1152−1161.

(133) Raimondi, P.; Benabderrahmane, C.; Berkvens, P.; Biasci, J. C.; Borowiec, P.; Bouteille, J.-F.; Brochard, T.; Brookes, N. B.; Carmignani, N.; Carver, L. R.; Chaize, J.-M.; Chavanne, J.; Checchia, S.; Chushkin, Y.; Cianciosi, F.; Di Michiel, M.; Dimper, R.; D'Elia, A.; Einfeld, D.; Ewald, F.; Farvacque, L.; Goirand, L.; Hardy, L.; Jacob, J.; Jolly, L.; Krisch, M.; Le Bec, G.; Leconte, I.; Liuzzo, S. M.; Maccarrone, C.; Marchial, T.; Martin, D.; Mezouar, M.; Nevo, C.; Perron, T.; Plouviez, E.; Reichert, H.; Renaud, P.; Revol, J.-L.; Roche, B.; Scheidt, K.-B.; Serriere, V.; Sette, F.; Susini, J.; Torino, L.; Versteegen, R.; White, S.; Zontone, F. The Extremely Brilliant Source Storage Ring of the European Synchrotron Radiation Facility. *Commun. Phys.* **2023**, *6* (1), No. 82.

https://doi.org/10.1021/photonsci.5c00051
Photon Sci. XXXX, XXX, XXX−XXX